International Journal of Immunopathology & Pharmacology

Original Research Article

Luteolin loaded on zinc oxide nanoparticles ameliorates non-alcoholic fatty liver disease associated with insulin resistance in diabetic rats *via* regulation of PI3K/AKT/FoxO1 pathway

International Journal of Immunopathology and Pharmacology
Volume 36: 1–16

DOI: 10.1177/03946320221137435
journals.sagepub.com/home/iji
SAGE

Esraa SA Ahmed, Hebatallah E Mohamed and Mostafa A Farrag

Abstract

Objective: Non-alcoholic fatty liver disease (NAFLD) is a worldwide health problem with high prevalence and morbidity associated with obesity, insulin resistance, type 2 diabetes mellitus (T2DM), and dyslipidemia. Nano-formulation of luteolin with Zn oxide in the form of Lut/ZnO NPs may improve the anti-diabetic property of each alone and ameliorate the insulin resistance thus management of NAFLD. This study aimed to measure the efficiency of Lut/ZnO NPs against insulin resistance coupled with NAFLD and T2DM.

Methods: A diabetic rat model with NAFLD was induced by a high-fat diet and streptozotocin (30 mg/kg I.P). Serum diabetogenic markers levels, lipid profile, and activity of liver enzymes were measured beside liver oxidative stress markers. Moreover, the hepatic expressions of PI3K/AKT/FoxO1/SERBP1c as well as heme oxygenase-1 were measured beside the histopathological examination.

Results: Lut/ZnO NPs treatment effectively reduced hyperglycemia, hyperinsulinemia, and ameliorated insulin resistance. Additionally, Lut/ZnO NPs improved the hepatic functions, the antioxidant system, and reduced the oxidative stress markers. Furthermore, the lipid load in the liver, as well as the circulating TG and TC, was minified *via* the suppression of lipogenesis and gluconeogenesis. Moreover, Lut/ZnO NPs activated the PI3K/AKT signaling pathway, hence inactivating FoxO1, therefore enhancing the hepatic cells' insulin sensitivity.

Conclusion: Lut/ZnO NPs have a hepatoprotective effect and may relieve the progression of NAFLD by alleviating insulin resistance, ameliorating the antioxidant status, and regulating the insulin signal pathway.

Keywords

luteolin/ ZnO NPs, insulin resistance, non-alcoholic fatty liver disease, type 2 diabetes mellitus, PI3K/AKT/FoxO1 signaling pathway

Date received: 8 June 2022; accepted: 20 October 2022

Introduction

The high prevalence (25–30%), morbidity, and mortality of the worldwide non-alcoholic fatty liver disease (NAFLD) were associated with the progression of many harmful and damaging complications in the liver tissues, including

Radiation Biology Research, National Center for Radiation Research and Technology, Egyptian Atomic Energy Authority, Cairo, Egypt

Corresponding author:
Esraa SA Ahmed, Radiation Biology Research, Egyptian Atomic Energy Authority, Nasr City, Cairo 11787, Egypt.
Emails: esraa.tamim@yahoo.com, esraa.tamim@eaea.org.eg

steatosis, non-alcoholic steatohepatitis, fibrosis, and cirrhosis, that ultimately develop hepatocellular carcinoma.[1,2] Hassan et al.[3] found that Egyptian prevalence of NAFLD was 15.8% among both children and adolescents which increases with age from (≤20 to more than 40%) under the age of 20 years to over the age of 60 years, respectively. Additionally, it is predominant in men (31%) more than in women (16%). It is characterized by the excessive aggregation and deposition of lipid content (≥5–10%) in the hepatocytes, consequently raising oxidative stress and free fatty acids leading to augment synthesis and accumulation of triglyceride.[4] The complicated pathogenesis of NAFLD was correlated to obesity, type 2 diabetes (T2DM), dyslipidemia, insulin resistance, mitochondrial dysfunction, endoplasmic reticulum stress, inflammation, gut microbiota disorders, and dietary factors.[5]

The liver is a vital organ that has an important role in many metabolic processes like glucose and lipid metabolism besides the skeletal muscle and adipose tissue.[6] The metabolic activity of the liver is regulated mainly by insulin through insulin signaling IRS/PI3K/AKT/FoxO1.[7] Besides that, it regulates the cell cycle, cell growth, and apoptosis.[8] Whereas dysregulation of the insulin signaling induces insulin resistance in which insulin lose its ability to control and regulate the hepatic metabolism of both glucose and lipid, leading to hyperglycemia (excessive glucose production) and hyperlipidemia (accelerated rates lipogenesis).[7]

Based on the strong link between NAFLD and T2DM, anti-diabetic medications can be used for the treatment of NAFLD.[9] But the oral antidiabetic drugs have adverse side effects, consequently, changing the lifestyle and consuming a diet rich in natural phytonutrients are effective in the management of diabetes and also for patients with NAFLD due to their various pharmacological activities.[10] Luteolin (3′, 4′, 5, 7-tetrahydroxy flavone) is a flavonoid derived from many traditional Chinese medicinal plants. It is widely present in many edible vegetables, like pepper, celery, carrot, and spinach.[11] Luteolin is known to have multiple health benefits including antioxidant potential,[12] anti-inflammatory effects,[13] hepatoprotective roles,[14] in addition to its anticancer and neuroprotective effects.[15] The anti-diabetic potential of luteolin was reported in several studies. Luteolin ameliorated hepatic/adipose tissue insulin resistance in diet-induced obesity complications.[16] Furthermore, Sangeetha[17] revealed that luteolin retained levels of blood glucose and ameliorated the sensitivity of body cells to insulin thus confirming its anti-diabetic effect. Additionally, luteolin influenced many disorders related to glycolipid metabolism in particular insulin resistance, and diabetes.[18] Moreover, Xiong et al.[19] reported that luteolin ameliorated lipid and glucose metabolism through control of the metabolic organs (hypothalamus, liver, and adipose tissue). Lin et al.[20] confirmed its role in the regulation of lipids by enhancing β-oxidation of fatty acids and lipolysis in neurons resulting from elevated serotonin. Additionally, Bumke-Vogt et al.[21] demonstrated that luteolin alleviated hepatic steatosis *via* inhibition of gluconeogenesis and lipogenesis. Furthermore, luteolin activated the hippocampal insulin signaling pAkt/glycogen synthase kinase (pGSK), hence increasing the infusion of glucose along with reducing hepatic glucose production.[22]

Nanoformulation of numerous nutraceutical compounds and even drugs overcome many limitations including solubility, bioavailability, and delivery of these compounds to their active site. Abd-Allah et al.[23] reported that nanoformulation of nicotinamide or ascorbic acid in chitosan nanoparticles improved their hepatoprotective effect and alleviated the NAFLD via modulation of the insulin resistant, oxidative stress status besides amelioration of hepatic function and lipid content. Moreover, Li et al.[24] indicated that encapsulation of modified glycogen polymer with resveratrol improved NAFLD by targeting the redox status and reducing fat accumulation in the liver tissues as well as liver injury. The bioavailability and therapeutic efficiency of Celastrol against NAFLD were enhanced via its incorporation with biodegradable albumin-based nanoparticles.[25]

Like many nutraceutical compounds, the low solubility of luteolin in water makes its intravenous or intraperitoneal administration very difficult and thus minified its bioavailability and efficiency.[18] Therefore, nano-formulation of luteolin as one of the phytochemicals improved its solubility, bioavailability, biodistribution, and potentiate its anti-diabetic effect.[26] Zinc (Zn) is a suitable choice because it is a trace element metal involved in glucose metabolism by improving the insulin signaling pathway and hepatic glycogenesis.[27] Moreover, zinc oxide nanoparticles (ZnO NPs) regulated blood glucose in diabetic rats due to their potent anti-diabetic effect by modulation of the glycemic parameters along with reducing the production of free radicals. Conclusively, nano-formulation of luteolin with Zn in the form of Lut/ZnO NPs may improve efficacy/bioavailability and enhance its delivery and thus augment the anti-diabetic effect.

Therefore, this study is designed to evaluate the effectiveness of Lut/ZnO NPs in ameliorating hyperlipidemia and diabetes-associated NAFLD and insulin resistance, particularly through its impact on PI3K/AKT/FoxO1 signaling pathway.

Materials and methods

Materials

Luteolin, Streptozotocin (STZ), and all chemicals used in this study were obtained from Sigma–Aldrich® (St Louis, Missouri, USA).

High-fat diet (HFD) was obtained from El-Nasr Co. (Cairo, Egypt), consisting of 45% carbohydrate, 20% protein, and 35% fat.

Luteolin/ZnO nano-dispersions preparation (Lut/ZnO NPs)

Luteolin/ZnO nano-dispersions was prepared first as a stock. A 0.5 g of luteolin was dissolved in 200 mL distilled water under heating for nearly 1 h. Then the obtained luteolin solution was left to settle and the supernatant was taken and stored for the next step. After that, 100 mL of luteolin solution was added to 100 mL of zinc acetate (1000 ppm) under vigorous stirring using a magnetic stirrer and heated at 80 ^{o} C. Next, 200 mL of NaOH (0.5 M) was added drop by drop wisely and slowly until the reaction is complete. Then, the solution was left to settle and washed several times with distilled water by decantation and the final solution reached 100 mL, then exposed to a dose of 10 KGy and placed in a clean bottle and sealed carefully until further use. The concentration of ZnO/Luteolin nanodispersions was calculated to be 0.006 g/mL.

Characterization of luteolin/ZnO nanodispersions

The morphology and size of the luteolin/ZnO nanodispersion (Lut/ZnO NPs) were analyzed by Transmission Electron Microscopy (TEM). The luteolin/ZnO nanodispersion was dried and placed on an ultra-thin carbon-supported Cu grid and examined by TEM (JEOL; model JEM100CS, Japan). Additionally, dynamic light scattering (DLS) was used to determine the particle size distribution *via* fluctuation of scattered light intensity by the particles in Brownian motion using the Zeta sizer. Moreover, the X-ray diffraction (XRD) spectrum was obtained using the XD-DI Series, and the Scherer equation was used to calculate the particle size of Lut/ZnO NPs. Additionally, the UV/Vis spectrum of luteolin and Lut/ZnO NPs samples of both were detected by Ultraviolet-Visible spectroscopy (T60 UV-Vis spectrophotometer) (PG instruments) at 190–1100 nm.

Determination of LD_{50} of Lut/ZnO NPs

In order to determine the optimal dose with no observed adverse effects, female rats were used to calculate the LD50 value of Lut/ZnO NPs according to the method of Reed and Muench[28] and Bass et al.[29] The median lethal dose (LD_{50}) of Lut/ZnO NPs was determined using a dose range from 1.2 to 120 mg/kg body weight. After 24°h, mortality was observed, and LD50 was calculated from the following equation:

$$\begin{aligned}\text{Log LD50} = {} & \text{Log LD next below 50\%} \\ & + (\text{Log increasing factor} \\ & \times \text{proportionate distance}).\end{aligned}$$

Proportionate distance

$$= \frac{50\,\% - \text{mortality next below 50\,\%}}{\%\ \text{mortality above 50\,\%} - \text{mortality next below 50\,\%}}$$

Experimental animals

Sixty male Wistar rats (12-month-old) weighing approximately 240–250 g were brought from the Egyptian National Authority for Drug Research and Control, Cairo, Egypt. During the experimental period, all rats had free access to food and water and were placed in identical laboratory conditions with a light/dark cycle of 12°h, humidity of 50 ± 15%, and temperature of 22 ± 2°C. The use of experimental animals has been handled under the standards and guidelines of the National Research Center Ethics Committee published by the U.S. National Health Institutes (NIH publication No. 85–23, 1996) and the National Research Center Ethics Committee. Additionally, it was approved by the Institutional Animal Care and Use Committee (Vet CU 2305 2022463)

Experimental groups

After the accommodation period, the rats were randomly classified into six groups (n = 10) as follows:

1. Normal control group: where the rats were fed with a normal rat diet and were injected with saline intraperitoneally.
2. Lut/ZnO NPs group: the rats were fed with a normal rat diet and were injected with Lut/ZnO NPs intraperitoneally at a dose of 12 mg/kg/body weight three times/week for 3 weeks.
3. HFD group: the rats fed on HFD for 12°weeks and did not receive any treatment
4. HFD+ Lut/ZnO NPs group: the rats were fed with HFD and treated with Lut/ZnO NPs as in group 2.
5. 5HFD+ STZ group: the rats received a single dose of STZ intraperitoneally (35 mg/kg body weight) dissolved in citrate buffer (pH 4.5).[30]
6. HFD+STZ+ Lut/ZnO NPs group: where the rats were injected with STZ, like group (5) and treated with Lut/ZnO NPs, like group (2).

After 3 days of the injection with STZ, an ACCU-CHEK glucometer was used to measure Fasting Blood

Glucose (FBG) levels to assure the induction of T2DM. The rats with FBG levels greater than or equal to 11.1 mmol/L (288 mg/dl) were counted as diabetics and were used to complete the experiment.

After the experimental period, all rats were sacrificed under diethyl ether anesthesia and the blood samples were gathered *via* cardiac puncture and divided into two tubes. One for plasma to measure the glucose levels, and the other one to obtain serum for further biochemical estimates. Liver tissues were separated immediately, washed with 0.9% physiological saline, and divided into two parts. The first part was used for the histological examinations, while the second one was stored at −80°C for further analysis.

Serum biochemical estimations

The FBG levels were measured with an ACCU-CHEK glucometer. A commercial ELISA kit (My Biosource Inc., San Diego California, USA) was used to quantify insulin levels in the serum. The homeostasis model assessment of insulin resistance (HOMA-IR) index is an indicator of insulin resistance. It was determined for each rat as follows: HOMA-IR = [fasting insulin (μU/ml) x fasting glucose (mmol/l)]/22.5.[31]

Estimation of liver function tests: Using the method of Reitman and Frankel,[32] the activity of both aspartate transaminase (AST) and alanine transaminase (ALT) were detected in serum.

Estimation of lipid parameters: The levels of Total Cholesterol (TC) and Triglycerides (TG) were measured in serum according to the method of Allain et al.,[33] and Fossati and Prencipe,[34] respectively, using a TC and TG kits purchased from Biodiagnostic Company. Moreover, according to the method of Lopes-Virella et al.,[35] levels of high-density lipoprotein cholesterol (HDL-C) were estimated. According to the method of **Zhou et al.** (36), the levels of free fatty acid in the liver tissues were determined.

Estimation of oxidative stress markers: Lipid peroxidation (malondialdehyde (MDA)),[37] reduced glutathione (GSH),[38] and oxide glutathione (GSSG)[39] levels were measured in the liver tissue. Additionally, using the method of Bełtowski et al.,[40] the activity of paraoxonase-1 was detected.

Molecular estimations (Reverse transcription-quantitative PCR (RT-qPCR). *Total* RNA was extracted from liver tissues using TRIzol reagent (Life Technologies, USA). The synthesis of the complementary DNA (cDNA) was done with reverse transcriptase. According to the manufacturer's protocol of SYBR Green PCR Master Mix (Applied Biosystems ^{TM}), the reaction reagents were added, the conditions were adjusted, and gene amplification was performed by PCR. The primer sequences were as follows: PDK1, F: 5′-AAGGGTACGGGCCTCTCAAA-3′ and R: 5′-CCCACGTGATGGACTCAAAGA-3′; G6pase, F: 5′-CGTCACCTGTGAGACTGGAC-3′ and R: 5′-ACGACATTCAAGCACCGGAA-3′; HO-1, F: 5′-CGACAGCATGTCCCAGGATT-3′ and R: 5′-TCGCTCTATCTCCTCTTCCAGG-3′ β-actin, F: 5′ CCAGGCTGGATTGCAGTT3′ and R: 5′GATCACGAGGTCAGGAGATG3. At the end of the reaction, the relative expression of the gene of interest was normalized to β-actin using the $2^{-\Delta\Delta Ct}$ method.[41]

Western blot analysis: The proteins were quantified using the Bradford method[42] and were isolated by10% SDS-PAGE and transferred onto polyvinylidene difluoride (PVDF) membranes. After that, the membranes were blocked with 5% skimmed milk and were incubated with primary antibodies to IRS, PI3K, AKT, SREBP1c, and FoxO-1(Cell Signaling Technologies, USA) overnight at 4°C. After washing, the membranes were exposed to the secondary monoclonal antibodies conjugated with horseradish peroxidase, and washed four times. The obtained immunoblots were visualized by chemiluminescence and X-ray film (Amersham detection kit). Moreover, proteins were quantified by a scanning laser densitometer (Biomed Instrument Inc., USA) and normalized for β- actin.

Histopathological examination of liver tissues. Liver tissues were fixed in a 10% buffered formalin solution and were embedded in paraffin by conventional methods. The tissues were cut into 3 μm sections and were stained with hematoxylin-eosin (H&E) stain. The stained sections were examined under a Light Microscope. According to the scale of Plaa et al.,[43] the severity of lesions in the hepatic tissues were classified into grade 0: Normal structure (no injury), grade I: Swelling of hepatocytes, grade II: Ballooning of hepatocytes, grade III: Lipid droplets in hepatocytes, and grade IV: Apoptosis and Necrosis of hepatocytes.

Statistical analysis

All data are expressed as the mean± SE. Using the statistical package SPSS software version 20, a one-way analysis of variance (ANOVA) followed by post-hoc multiple comparisons (LSD test) was used to evaluate the difference between groups at P-value <0.05 which is statistically significant. The charts were graphed *via* GraphPad Prism 8 (GraphPad, CA, USA).

Results

Using nanotechnology, luteolin which is hydrophobic was loaded on ZnO NPs to boost the bioavailability and solubility of luteolin as well as enhance its delivery and potentiate the therapeutic efficiency.

Characterization of Lut/ZnO NPs

As illustrated in Figure 1, the properties of Lut/ZnO nanodispersions were characterized by TEM, DLS, and XRD to give the size of each preparation. The size and morphology of the obtained Lut/ZnONPs were further confirmed by TEM studies. As shown in Figure 1(a), the TEM analysis of Lut/ZnONPs confirms that the particles reported here were almost hexagonal with particle sizes of approximately 17 nm. DLS analysis displayed that the mean size of the nanoparticles was about 172.6 nm as shown in Figure 1(b). XRD is used to confirm the formation and presence of ZnO nanoparticles, also to measure the particle size of the formed nanoparticles. Moreover, the XRD pattern of ZnO is shown in Figure 1(c) and the strong Bragg Reflection peaks at ($2\theta = 32.6°$, 35.5°, 37.2°, 48.2°, 57.3°, 63.5°, 68.8°, and 70.1°), matched by their Miller indices ((100), (002), (101), (102), (110), (103), (112), and (004)), were obtained from a standard wurtzite ZnO structure (JCPDS Card No. 36–1451) Therefore, hexagonally structured ZnO was identified as a single crystalline phase in the Lut/ZnO nanoparticles with a mean particle size of 174.7 nm in agreement with the results obtained from the DLS particle size distribution of Lut/ZnO nanodispersion. UV-vis spectroscopic analysis of both ZnO NPs and Lut/ZnO nanodispersion showed the absorbance maxima from the phenyl rings of luteolin at about 340 and 390 nm (Figure 1(d).

LD50 of Lut/ZnO NPs

The results of the LD_{50} of the prepared Lut/ZnO NPs showed that the safe dose for the intraperitoneal (ip) injection was 12 mg/kg b wt, indicating the safety and absence of harmful effects of the Lut/ZnO NPs.

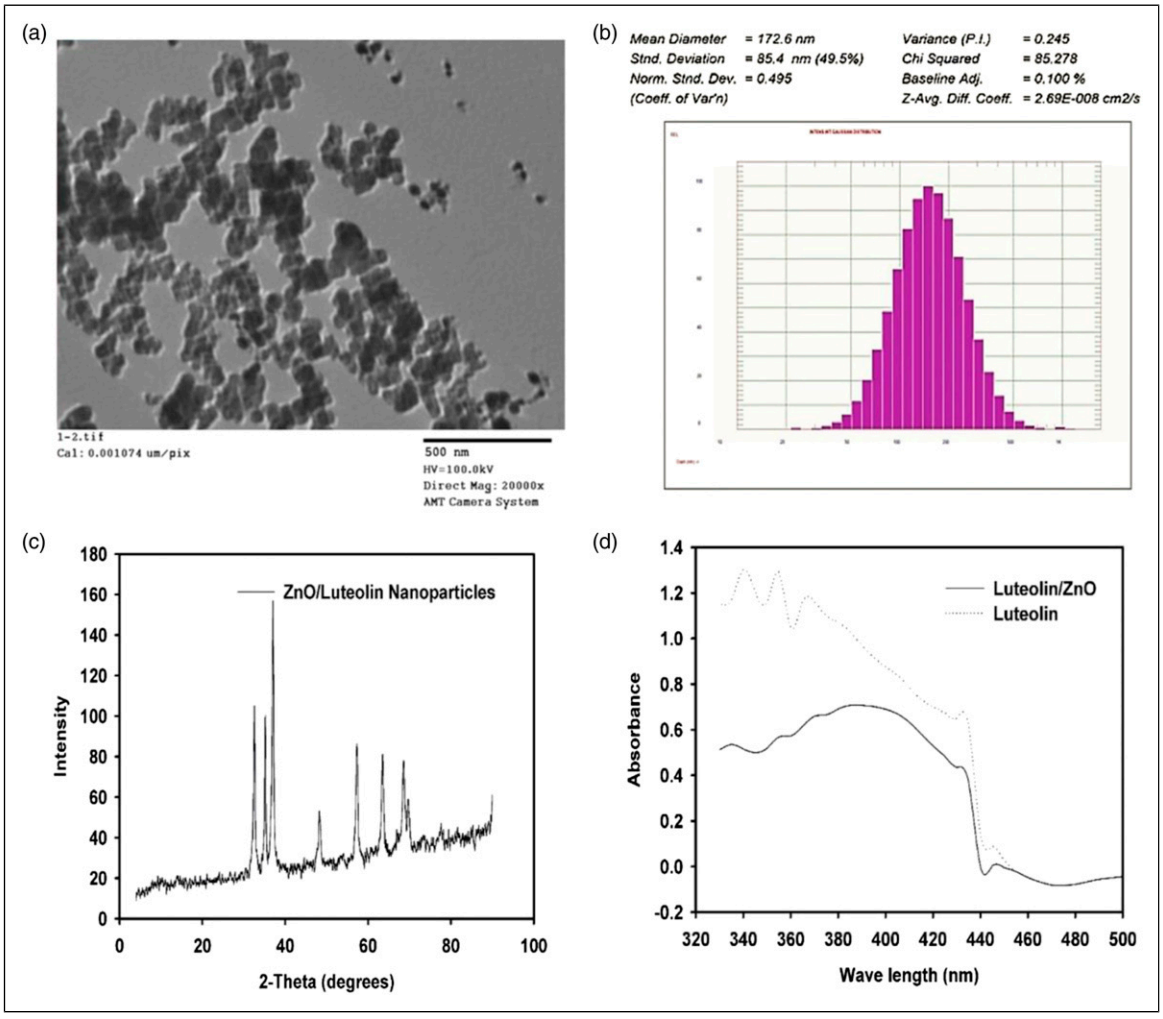

Figure 1. Characterization of Lut/ZnO NPs. (a): TEM, (b): DLS analysis of Lut/ZnO NPs size distribution, (c): XRD pattern of Lut/ZnO nanoparticles and (d): UV spectra of pure luteolin and ZnO/Luteolin nanodispersion.

Effects of Lut/ZnO NPS on the blood glucose, insulin levels, and insulin resistance

Results in Figure 2 illustrated that the 12 weeks of the HFD feeding and injection with STZ resulted in a significant increase in FBG, fasting blood insulin, as well as HOMA-IR index ($p < 0.05$), which confirmed the induction of diabetes and insulin resistance in rats. However, the levels of FBG, insulin, and HOMA-IR were remarkably reduced upon treatment with Lut/ZnO NPs. These results suggest that Lut/ZnO NPs effectively ameliorated the glucose tolerance and insulin sensitivity in HFD-induced obesity and HFD+STZ-induced T2DM in rats, thus confirming the antidiabetic potential of the Lut/ZnO NPs.

Effect of Lut/ZnO NPs on the insulin signaling pathway

To evaluate whether Lut/ZnO NPs reduced the blood glucose and improved insulin resistance through PI3K/AKT pathway, the expressions of IRS, PI3K, AKT, andFoxO1 in liver tissues were detected by western blot. Whereas the PCR was used to detect the expression of PDK1 and G6Pase in liver tissue. The current results reported that the expressions of IRS, PI3K/PDK1, and AKT levels were significantly downregulated along with the upregulation of FoxO1 (activate dephosphorylated form) and its downstream G6Pase in both obese and T2DM groups relative to the control group. In contrast, Lut/ZnO NPs treatment efficiently triggered the insulin signaling pathway *via* upregulating the expression of IRS, PI3K, and AKT) when compared to the obese and T2DM groups. Furthermore, the upregulated expressions of both FoxO1 and G6Pase were notably reversed upon treatment with Lut/ZnO NPs as shown in Figure 3.

Effect of Lut/ZnO NPs on lipogenesis (SREBP1c)

Sterol regulatory element-binding protein 1c (SREBP1c) is the master regulator of lipid and cholesterol metabolism. Both HFD and HFD+STZ elevated the expression of SREBP1c protein as compared to the control group. In contrast, treatment with Lut/ZnO NPs showed an opposite effect through downregulating the SREBP1c expression as shown in Figure 4.

Effect of Lut/ZnO NPs on serum lipid profile

Additionally, as shown in Table 1, the levels of the blood lipids including TC and TG were higher, whereas the HDL-C was significantly decreased in both HFD and HFD+STZ groups compared to the control group. Moreover, the levels of TG and FFA in the liver tissues were significantly increased in the HFD and HFD+STZ groups. However, treatment with Lut/ZnO NPs diminished the hyperlipidemia associated with HFD and T2DM *via* reducing the levels of TC, and TG (in serum and liver tissues) as well as FFA and increasing that of HDL-C. This may suggest the anti-hyperlipidemic effect of Lut/ZnO NPs, which would improve insulin resistance indirectly. Therefore, lowering serum lipids will reduce the hepatic accumulation of fatty acids and triglycerides.

Effect of Lut/ZnO NPs on hepatic oxidative stress

NAFLD patients and animal models were coupled with an increment in lipid peroxidation and a decline in the

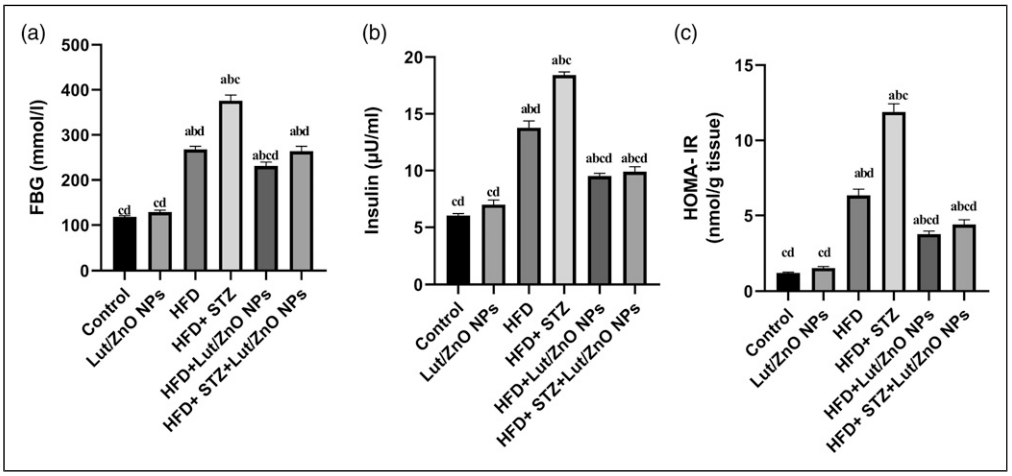

Figure 2. Effect of Lut/ZnO NPs on diabetic parameters: FBG (a), insulin (b), and HOMA-IR (c). Values were expressed as Means ± SE ($n = 6$). a: denote significant change versus control, b: denote significant change versus Lut/ZnO NPs, c: denote significant change versus HFD and d: denote significant change versus HFD+STZ at $p < 0.05$.

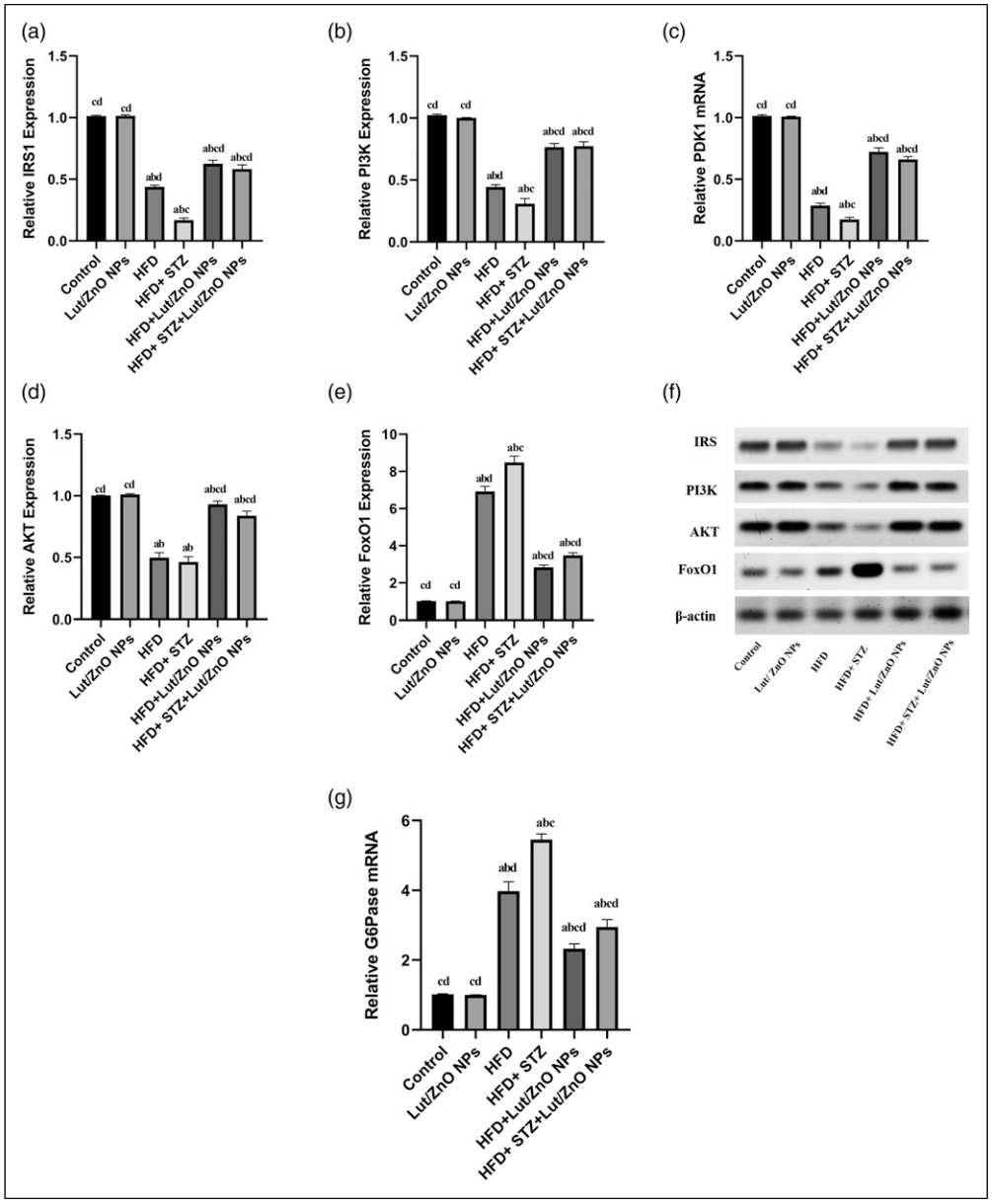

Figure 3. Effects of Lut/ZnO NPs on IRS, PI3K, PDK1, AKT, FoxO1 and G6Pase expression in hepatic tissues of NAFLD rat model. Quantitative western blotting analysis of IRS (a), PI3K (b), AKT (d), FoxO1 (e), and β-actin protein level. Western blotting of IRS, PI3K, AKT, FoxO1, and β-actin (f). Moreover, the gene expression of PDK1 (c) and G6Pase (g) was represented. Values were expressed as Means ± SE (n = 6). a: denote significant change versus control, b: denote significant change versus Lut/ZnO NPs, c: denote significant change versus HFD and d: denote significant change versus HFD+STZ at $p < 0.05$.

antioxidant content. Insulin resistance and dyslipidemia in liver tissues are linked with mitochondrial dysfunction and impairment in the redox status. The obtained results in Table 2 showed a notable elevation in the MDA, and GSSG levels accompanied with a marked decline in the GSH level and paraoxonase-1 activity within the liver tissues in both HFD and T2DM groups compared with the control groups. Moreover, a remarkable decline in the hepatic gene expression of homooxygenase-1 in both HFD and T2DM groups was observed compared with the control groups (Figure 5). However, treatment with Lut/ZnO NPs caused a significant reduction in the level of MDA and GSSG in both HFD and HFD+STZ groups. Moreover, the content of GSH and the expression of

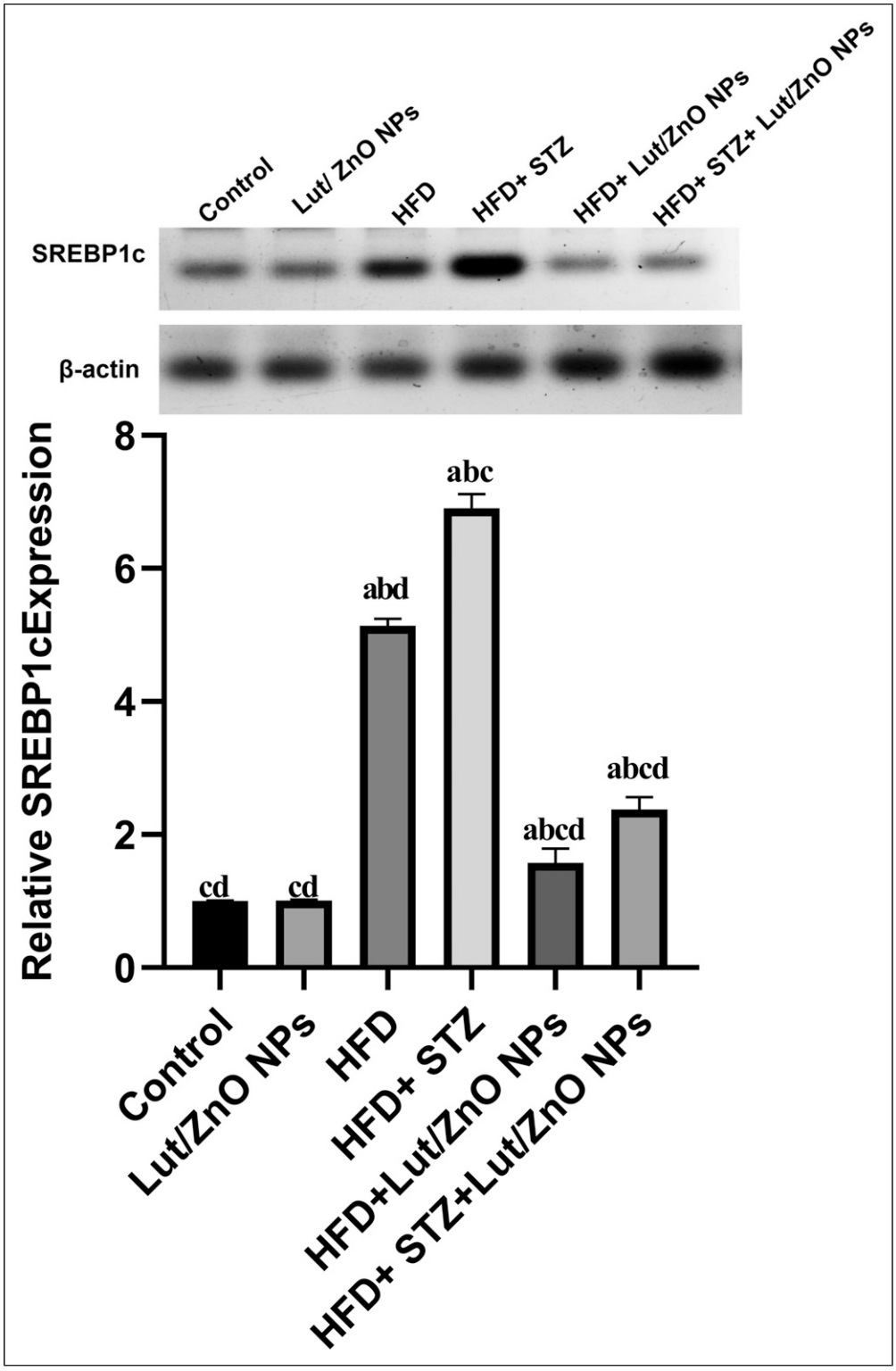

Figure 4. Effects of Lut/ZnO NPs on SREBP1c protein expression in hepatic tissues of NAFLD rat model. Values were expressed as Means ± SE (n = 6). a: denote significant change versus control, b: denote significant change versus Lut/ZnO NPs, c: denote significant change versus HFD and d: denote significant change versus HFD+STZ at $p < 0.05$.

Table 1. Effect of Lut/ZnO NPs on serum lipid parameters.

Groups	Parameters				
	TC (mg/dl)	TG_s (mg/dl)	TG_t (mg/g)	HDL-C (mg/dl)	FFA (mg/g)
Control	132.5 ± 24[a,b,c]	80.4 ± 4.5[a,b,c]	6.2 ± 0.14[a,b,c]	58.6 ± 2[a,b,c]	1.32 ± 0.06[a,b,c]
Lut/ZnO NPs	130.7 ± 1.7[b,c,d]	72.1 ± 3.2[b,c,d]	6.1 ± 0.04[b,c,d]	62.5 ± 1.7[b,c,d]	1.62 ± 0.7[b,c,d]
HFD	233.5 ± 3.8[a,d,c]	140.3 ± 1.7[a,d,c]	9.1 ± 0.06[a,d,c]	35.3 ± 1.6[a,d,c]	4.13 ± 0.03[a,d,c]
HFD+STZ	273.7 ± 8.4[a,b,d]	167.3 ± 1.9[a,b,dc]	9.5 ± 0.09[a,b,d]	28.5 ± 2.4[a,b,d]	6.4 ± 0.19[a,b,d]
HFD+Lut/ZnO NPs	186.4 ± 2.9[a,b,c,d]	97.1 ± 1.9[a,b,c,d]	7.07 ± 0.06[a,b,c,d]	46.7 ± 1.4[a,b,c,d]	3.1 ± 0.14[a,b,c,d]
HFD+STZ+Lut/ZnO NPs	181.9 ± 2.6[a,b,c,d]	92.4 ± 1.6[a,b,c,d]	7.2 ± 0.16[a,b,c,d]	57.8 ± 2.5[a,b,c,d]	2.3 ± 0.19[a,b,c,d]

Triglycerides (TG) in serum (TG_s) and liver tissue (TG_t), total cholesterol (TC) and high-density lipoprotein cholesterol (HDL-C) contents. Values were expressed as Means ± SE (n = 6).
[a]denote significant change versus Lut/ZnO NPs.
[b]denote significant change versus HFD.
[c]denote significant change versus HFD+STZ at $p < 0.05$.
[d]denote significant change versus control.

Table 2. Effect of Lut/ZnO NPs on hepatic oxidative stress status.

Groups	Parameters			
	MDA (nmol/g tissue)	GSSG (nmol/g tissue)	GSH (nmol/g tissue)	PON1 (U/mg tissue)
Control	38.2 ± 2.7[a,b,c]	42.1 ± 1.4[a,b,c]	97.2 ± 1.4b[a,b,c]	63.37 ± 2.1[a,b,c]
Lut/ZnO NPs	32.7 ± 1.7[b,c,d]	36.3 ± 2.3[b,c,d]	107.5 ± 1.5[b,c,d]	73.35 ± 1.5[b,c,d]
HFD	104.6 ± 5.8[a,d,c]	93.7 ± 1.9[a,d,c]	48.8 ± 2.9[a,d,c]	39.25 ± 1.3[a,d,c]
HFD+STZ	129.1 ± 3.0[a,b,d]	103.5 ± 3.7[a,b,d]	32.1 ± 1.3[a,b,d]	27.82 ± 2.6[a,b,d]
HFD+Lut/ZnO NPs	68.1 ± 3.9[a,b,c,d]	63.6 ± 3.7[a,b,c,d]	74.9 ± 1.6[a,b,c,d]	52.8 ± 1.0[a,b,c,d]
HFD+STZ+Lut/ZnO NPs	77.5 ± 4.2[a,b,c,d]	58.7 ± 1.8[a,b,c,d]	64.6 ± 2.1[a,b,c,d]	55.75 ± 1.2[a,b,c,d]

Values were expressed as Means ± SE (n = 6).
[a]denote significant change versus Lut/ZnO NPs.
[b]denote significant change versus HFD.
[c]denote significant change versus HFD+STZ at $p < 0.05$.
[d]denote significant change versus control.

HO-1 were significantly increased after treatment with Lut/ZnO NPs.

Effect of Lut/ZnO NPs on hepatic dysfunction

As shown in Figure 6, both HFD and HFD+STZ groups revealed dramatical increase in the ALT and AST activities compared with the control group. This indicated hepatic damage. However, treatment with Lut/ZnO NPs significantly reversed the deterioration in the activities of the hepatic enzymes, suggesting that Lut/ZnO NPs may have a hepatoprotective role.

Histopathological examination

The photomicroscopic image of both the control and Lut/ZnO NPs groups' hepatic tissue section showed normal histological architecture of the liver (grade 0) (Figure 7 (a) and (b)). Meanwhile, the histopathological examination of hepatic tissues of the animals fed on HFD showed abundant fatty deposition in the hepatocytes forming signet ring cells that appeared as clusters scatter all over the hepatic lobules. Centrilobular coagulative necrosis of hepatocytes besides the hepatic cords mess and hyperplasia of Kupffer cells were found (grade IV) (Figure 7(c)). Similarly, the hepatic section of the HFD+STZ group showed severe damage to the hepatic lobules and fatty degeneration of hepatocytes, especially in the peripheral zone. Moreover, the hepatic parenchyma exhibited the perturbation of the hepatic cords and hyperplasia of Kupffer cells along with hepatocytes necrosis and dilatation of hepatic sinusoids (grade IV) (Figure 7(e)). On contrary, treatment of HFD with Lut/ZnO NPs resulted in restoring the regular arrangement of hepatic cords with some dilatation of hepatic sinusoids, binucleated cells, and hyperplasia of Kupffer cells (grade I) (Figure 7(d)). Additionally, the diabetic rats treated with Lut/ZnO NPs showed amelioration of the hepatic damage with the presence of a lower number of intracellular micro-vesicular steatosis, hyperplasia of Kupffer cells, and dilation of hepatic sinusoids (grade III) (Figure 7(f)).

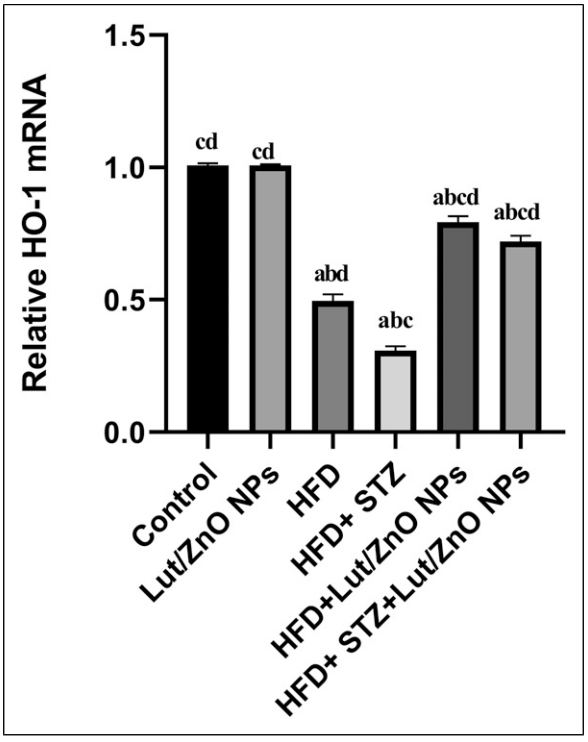

Figure 5. Effects of Lut/ZnO NPs on rat liver mRNA expression of HO-1 genes. Values were expressed as Means ± SE ($n = 6$). a: denote significant change versus control, b: denote significant change versus Lut/ZnO NPs, c: denote significant change versus HFD and d: denote significant change versus HFD+STZ at $p < 0.05$.

Discussion

Glucotoxicity or hyperglycemia associated with T2DM led to insulin resistance which is involved in the NAFLD pathogenesis.[44] It promoted the progression of NAFLD by increasing the contents of fatty acids in the liver, triggering hepatocellular dysfunction, inflammation, oxidative stress, and impaired the insulin signaling pathway. Moreover, it deranged insulin inhibition of hepatic glucose production and affected insulin sensitivity in muscle and adipose tissue.[9,45]

Consequently, the obtained results revealed that feeding rats with HFD and injection with STZ impaired glucose homeostasis, lipid metabolism, and tissue insulin sensitivity. This was evident *via* the higher levels of blood glucose (hyperglycemia) and insulin (hyperinsulinemia), and the increased value of HOMA-IR confirming the insulin resistance status in both HFD (obese) and HFD/STZ (diabetic) rats. These results are parallel to that of Mahmoud et al.[46] It was reported that Vornoli et al.[47] established a NAFLD model in rats using both HFD and low-dose STZ.

Consistently, the previous studies confirmed the strong connection between obesity, diabetes, and NAFLD in addition to insulin resistance, where the higher incidence of NAFLD was in both obese and diabetic.[48] Moreover, any defect in the insulin pathways and metabolism leads to insulin resistance and T2DM coupled with a higher risk of NAFLD progression.[49]

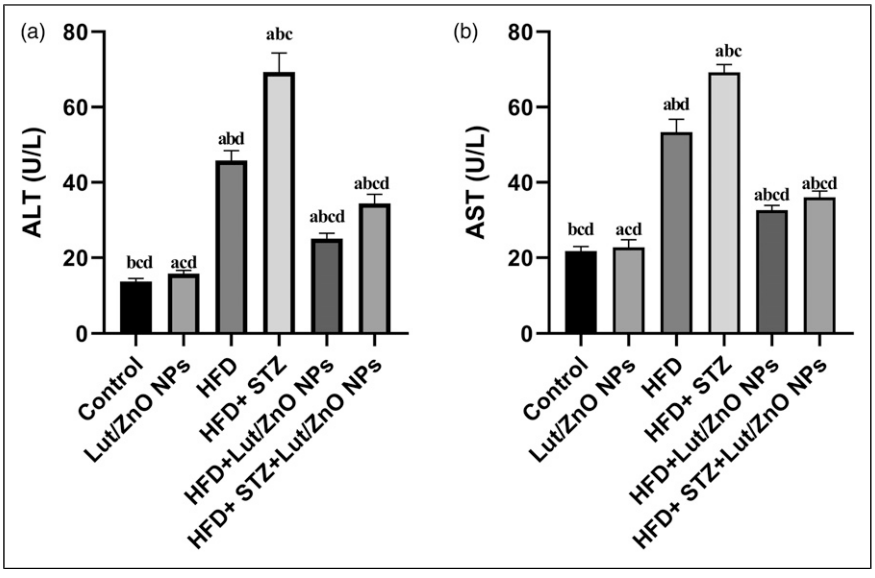

Figure 6. Effects of Lut/ZnO NPs on the liver enzymes, ALT (a) and AST (b). Values were expressed as Means ± SEM ($n = 6$). a: denote significant change versus control, b: denote significant change versus Lut/ZnO NPs, c: denote significant change versus HFD, and d: denote significant change versus HFD+STZ at $p < 0.05$.

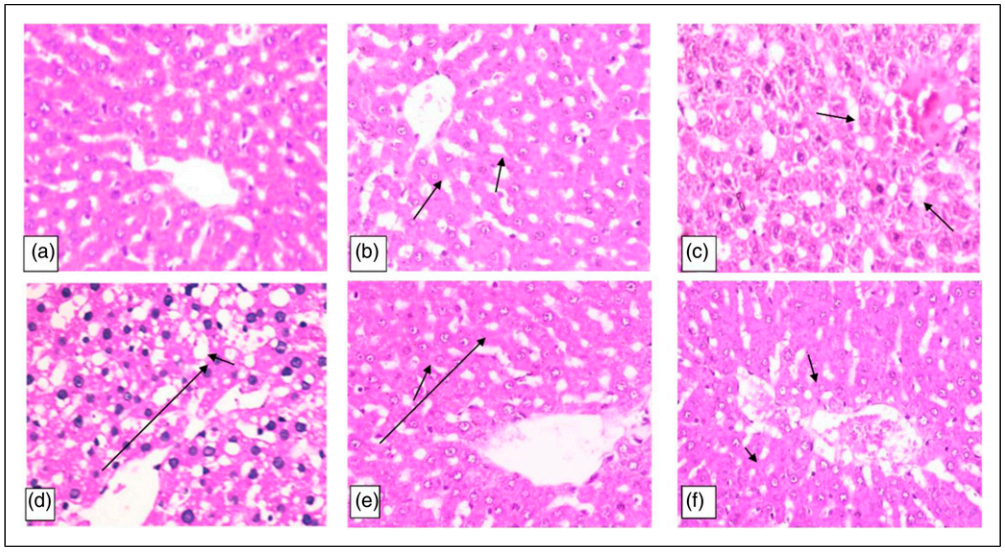

Figure 7. Photomicrograph of the hepatic tissue section. Figures (a and b) representing control and Lut/ZnO NPs showed a normal histological structure of the liver. However, Figure (c) (HFD) showed centrilobular coagulative necrosis of hepatocytes arrow. Figure (d) (HFD+ STZ) showed disorganization of hepatic cords, fatty degeneration, and necrosis of hepatocytes arrow. Lut/ZnO NPs treatment exhibited moderate hepatocytes swelling arrow (Figure (e)) and few numbers of intracellular microvesicular steatosis arrow (Figure (f)) representing the HFD+ Lut/ZnO NPs and HFD+ STZ+ Lut/ZnO NPs respectively (H&Ex200).

Thus, hyperinsulinemia in NAFLD is related to the defective clearance but not to secretion of insulin,[50] whereas hyperglycemia resulted as a consequence of the impaired insulin signaling pathway and IR.

In this respect, our results showed a remarkable defect in the insulin signaling pathway manifested by the down-regulated expression of IRS, PI3K, PDK1, and AKT with a concomitant upregulated expression of the nuclear FoxO1 which in turn activated the G6Pase a downstream target that promoted gluconeogenesis. These results agree with that of both Dwivedi et al.[30] and Lopes et al.[51] who reported that the status of insulin resistance is accompanied with the inhibition of the PI3K/AKT through FOXO1 activation promoting gluconeogenesis and thus hyperglycemia. Furthermore, Li et al.[8] reported that the protein levels of PI3K and Akt in the liver of NAFLD were decreased while their activation would promote liver regeneration and suppress the progression of NAFLD.

Conversely, following the treatment with Lut/ZnO NPs, the IRS/PI3K/AKT/FoxO1 was activated *via* upregulation of the phosphorylated levels of IRS, PI3K, and AKT in addition to increasing the PDK1 gene expression. This activation stimulated the phosphorylation of FoxO1, inhibiting its nuclear translocation and transcriptional function which subsequently diminished gluconeogenesis *via* downregulating the gene expression of the G6Pase. Supporting these results, Metallo et al.,[52] Guo,[53] and Gu et al.[54] all reported that the activation of the PI3K/AKT signaling pathway inactivated FoxO1 and inhibits G6Pase expression and increased hepatic glucose uptake, therefore improving the glucose tolerance and the responsiveness of both hepatic and adipose tissue to the insulin action as well as the protection of tissue from damage and failure.

According to the previous results, luteolin mediated its anti-diabetic effect by regulating the glucose levels in the blood and enhancing the insulin sensitivity and responsiveness of the tissues *via* the modulation of the insulin signaling pathway (IRS/AKT) and amelioration of the insulin sensitivity.[17,55] Additionally, Umrani and Paknikar[27] declared that the hypoglycemic effect of ZnO NPs was *via* suppression of gluconeogenesis, hence increasing the hepatic uptake and storage of glucose. Abdulmalek et al.[56] revealed that ZnO NPs significantly upregulated the phosphorylation of the IRS1/PI3K/AKT proteins. Therefore, based on the above-mentioned data, treatment with the Lut/ZnO NPs have a higher anti-diabetic efficiency due to the synergistic effect of luteolin and ZnO NPs.

Despite hyperinsulinemia, the insulin fails to control the hepatic metabolism, stimulating the excessive hepatic production of glucose (gluconeogenesis) via IRS/PI3K/PKB/FoxO1 even with the continuous lipid synthesis (lipogenesis) via SREBP1c leading to hyperglycemia and hyperlipidemia. This condition is known as selective hepatic insulin resistance.[7] Hardy et al.[57] showed that NAFLD was linked to dyslipidemia (dysregulated lipid metabolism) together with extreme deposition of different types of lipids, especially triglycerides.

Herein, there is a notable upregulation in the expression of SREBP-1c protein in the hepatic tissues of the HFD and HFD/STZ rats (both obese and diabetic rats). Additionally, it was found that hyperglycemia activated lipogenesis *via* carbohydrate responsive element-binding protein (ChREBP), a transcriptional factor that enhanced both lipogenesis and glycolysis lipogenesis along with hyperinsulinemia *via* SREBP1c which activated downstream lipogenic enzymes involved in hepatic lipogenesis.[58] Parallel to these results, Sanders et al.[59] indicated that insulin signaling increased the levels of SREBP1c in NAFLD.

Furthermore, Li et al.[60] confirmed that the higher SREBP-1c enhanced the synthesis and deposition of fatty acid and TG in the hepatic cells. Moreover, the obtained data showed remarkably increased levels of both TG and TC coupled with a decreased level of HDL-cholesterol. Consistent with the current results, Poulsen et al.[61] and Sun et al.[62] reported an elevation of the TG, VLDL-C, TC, LDL-C, and decreased HDL-C in dyslipidemia and NAFLD. Berlanga et al.[63] showed that the elevated levels of TG and TC were due to the insulin resistance status which enhanced the lipolysis of the peripheral adipose tissue and elevated the circulating free fatty acid flux to more than 59% which becomes the major origin of lipid delivered to the liver leading to the steatosis. Moreover, about 15% were derived from the ingestion of a fatty diet and 30% of the TG arose from *de novo* lipogenesis through the dysregulation in SREBP-1c- and FoxO-mediated hepatic insulin signaling.[64,65]

On contrary, Lut/ZnO NPs mitigated dyslipidemia in our result. Herein, Lut/ZnO NPs suppressed lipogenesis through the downregulation of SREBP1c which consequently reduced the levels of triacylglycerol and total cholesterol levels and enhanced that of the high-density lipoprotein cholesterol. Such results agreed with that of Liu et al.[66] and Zang et al.[67] who indicated that luteolin diminished the lipid accumulation in hepatocytes *via* the suppression of SREBP-1c and lipogenesis. Additionally, suppressing gluconeogenesis and restoring the insulin sensitivity of the body cells by luteolin prevented peripheral lipolysis decreasing the circulating levels of triglyceride and total cholesterol levels, thus reducing lipid delivery to the liver and alleviating hepatic steatosis.[16,17]

Previous studies reported the hypolipidemic effect of Zn and its synthesized ZnO NPs. Zinc regulated cellular physiology via modulation of the energetic metabolism (lipid and carbohydrate metabolism).[68] Wei et al.[69] showed that Zn supplementation reduced the lipid content in the hepatocytes by activating the oxidation of the free fatty acids and inhibiting lipogenesis. Moreover, it was found that Zn as well as ZnO NPs effectively reduced the levels of TC, TG, and LDL and increased the HDL in diabetic patients[70] and rats with HCC.[71] Notably, John et al.[72] confirmed the hypolipidemic potential of the ZnO nanoparticles, which may be attributed to behaving like insulin in the affected tissues, especially the pancreas[56] or its incorporation with the metalloenzymes that are responsible for lipid metabolism, thus inhibiting lipid biosynthesis.[73] Additionally, it was reported that ZnO NPs ameliorated the hepatic steatosis accompanied with insulin resistance by holding the SREBP-1c in the cytosol and preventing its nuclear translocation, thus hindering lipogenesis.[74] Collectively, ZnO nanoparticles hampered lipid accumulation in the hepatocytes by regulating pathways involved in lipid metabolism.

Considering hyperglycemia and dyslipidemia, the current data showed impairment in hepatic function and redox status. The hepatic lipotoxicity was coupled with a remarkable raise in the activity of the hepatic enzymes (ALT and AST) confirmed by the histopathological changes in the liver tissue. The nonalcoholic fatty liver is represented by disorganization of the liver architecture, hepatocyte injury, excessive fat deposition, and steatosis. These results coincide with that of Cheraghpour et al. [75] who pointed out that the hepatic injury and altered hepatic enzymes were attributed to dyslipidemia. Moreover, Raza et al.[76] and ALTamimi et al.[77] indicated that lipotoxicity induced mitochondrial β-oxidation, oxidative stress, and release of ROS that provoke liver damage. Similar to this, a marked increment in the lipid peroxidation and oxidized glutathione coupled with a sharp drop of the GSH content, and the activity of paraoxonase 1 (PON1) and hemeoxygenase-1 (HO-1) expression, were noticed in the current study. Moreover, Ağgül et al.[78] confirmed the depletion of the antioxidant content and excessive production of ROS in the diabetic model. Paraoxonase 1 (PON1) is a high-density lipoprotein (HDL) an associated enzyme involved in the protection of low-density lipoprotein and HDLs against lipid peroxidation.[79] However, the decreased activity of the PON1 in a diabetic model resulting from the impaired redox status is associated with plasma membrane injury and dysfunctional HDL.[80]

Conversely, Lut/ZnO NPs with their hypoglycemic efficiency and suppressive effect on lipogenesis alleviated the hepatic lipotoxicity and damage, and attenuated liver functions by hindering the activities of the hepatic enzymes together with ameliorating the histology of the liver manifested by restoring the normal architecture. Regarding the potential antioxidant effect of ZnO NPs and luteolin, the synergetic effect of both the form of Lut/ZnO NPs controlled the impaired redox status and replenished the depleted antioxidant contents in the hepatic tissues. As shown in the results, upon treatment with Lut/ZnO NPs, the levels of lipid peroxidation and the oxidized glutathione declined together with the enhancement in the antioxidant status (GSH, HO-1, and PON1).

The previous results revealed that luteolin with its lipid-lowering effect besides its potent antioxidant effect reduced

hepatic damage and dysfunction due to stabilization of plasma membrane and repairing the damaged hepatic tissue.[81] Additionally, Sangeetha[17] indicated that luteolin diminished ROS production *via* scavenging and suppression of the ROS-generating enzymes and pathways together with restoring the antioxidant content. Moreover, it alleviated diabetic nephropathy *via* increasing the HO-1 and AKT expressions. Similarly, the antioxidant efficiency of ZnO NPs was indicated in numerous studies, by their ability to scavenge free radicals and reduce ROS generation,[82] they can prevent oxidative cell damage and death induced by H_2O_2, hence alleviating the structural damage of the hepatic cells and improving hepatic function.[56] Moreover, ZnO NPs maintained the activity of paraoxonase in plasma.[83] Consequently, ZnO NPs alleviated the oxidative stress via their antioxidant, hypoglycemic, and hypolipidemic effects. Unfortunately, one of the limitations of this study is the absence of the sample size calculation in addition to the unavailability to perform histopathological analysis with the oil red staining for the liver tissue, which confirms the development of the NAFLD.

Conclusion

In conclusion, our results showed that the Lut/ZnO NPs substantially alleviated the hepatic injury and reduced the oxidative stress markers. Furthermore, the lipid load in the liver was diminished by lowering the levels of TG and TC besides suppressing lipogenesis and gluconeogenesis. Moreover, Lut/ZnO NPs activated the PI3K/AKT/FoxO1 signaling pathway, therefore improving the hepatic cells' insulin sensitivity. Consequently, Lut/ZnO NPs have a therapeutic effect on NAFLD and reduce its progression through their antioxidant, anti-diabetic, and lipid-lowering effects, besides regulating the insulin signal pathway in HFD/STZ-induced NAFLD in rats. However, further clinical estimations are needed to determine the potential mechanisms against liver disease.

Acknowledgments

For our assistance in the Luteolin/ZnO Nano-dispersions preparation, we thank associated professor Dr. Faten Ismail Abou El Fadl, Polymer Chemistry Department, National Center for Radiation Research and Technology (NCRRT), Egyptian Atomic Energy Authority.

We thank Prof. Dr. Ahmed Osman (professor of Pathology, Faculty of Veterinary Medicine, Cairo University) for his assistance in the histopathological assessment.

Declaration of conflicting interests

The author(s) declared no potential conflicts of interest with respect to the research, authorship, and/or publication of this article.

Funding

The author(s) received no financial support for the research, authorship, and/or publication of this article.

Ethics approval

The use of experimental animals has been handled under the standards and guidelines of the National Research Center Ethics Committee published by the U.S. National Health Institutes (NIH publication No. 85–23, 1996) and the National Research Center Ethics Committee. Additionally, it was approved by the Institutional Animal Care and Use Committee (Vet CU 2305 2022463).

Animal welfare

The present study followed international, national, and/or institutional guidelines for animal treatment and complied with relevant legislation

Availability of data and materials

All data obtained from this study are included in the current manuscript.

ORCID iD

Esraa SA Ahmed https://orcid.org/0000-0001-5358-4394

References

1. Rafiei H, Omidian K and Bandy B (2017) Comparison of dietary polyphenols for protection against molecular mechanisms underlying nonalcoholic fatty liver disease in a cell model of steatosis. *Molecular Nutrition & Food Research* 61: 1600781. DOI: 10.1002/mnfr.201600781.
2. Sabir U, Irfan HM, Alamgeer UA, et al. (2022) Reduction of hepatic steatosis, oxidative stress, inflammation, ballooning and insulin resistance after therapy with safranal in NAFLD animal model: a new approach. *Journal of Inflammation Research* 15: 1293–1316. DOI: 10.2147/JIR.S354878.
3. Hassan AM, Elhaw MH, Ahmed AA, et al. (2020) Value of screening for nonalcoholic fatty liver disease in hyperuricemic patients with normal body mass index by two-dimensional ultrasound: upper Egypt experience. *Al-Azhar Assiut Medical Journal* 18: 104–109. http://www.azmj.eg.net/text.asp?2020/18/1/104/281346
4. Donaldson J, Ngema M, Nkomozepi P, et al. (2019) Quercetin administration post-weaning attenuates high-fructose, high-cholesterol diet-induced hepatic steatosis in growing, female, Sprague Dawley rat pups. *Journal of the Science of Food and Agriculture* 99: 6954–6961.
5. Liu X, Sun R, Li Z, et al. (2021) Luteolin alleviates non-alcoholic fatty liver disease in rats via restoration of intestinal mucosal barrier damage and microbiota imbalance involving

in gut-liver axis. *Archives of Biochemistry and Biophysics* 711: 109019. DOI: 10.1016/j.abb.2021.109019.
6. Rui L (2014) Energy metabolism in the liver. *Comprehensive Physiology* 4(1): 177–197. DOI: 10.1002/cphy.c130024.
7. Santoleri D and Titchenell PM (2019) Resolving the paradox of hepatic insulin resistance. *Cell Mol Gastroenterol Hepatol* 7(2): 447–456. DOI: 10.1016/j.jcmgh.2018.10.016.
8. Li S, Wang X, Zhang J, et al. (2018a) Exenatide ameliorates hepatic steatosis and attenuates fat mass and FTO gene expression through PI3K signaling pathway in nonalcoholic fatty liver disease. *Brazilian Journal of Medical and Biological Research* 51(8): e7299. DOI: 10.1590/1414-431x20187299.
9. Tomah S, Alkhouri N and Hamdy O (2020) Nonalcoholic fatty liver disease and type 2 diabetes: where do diabetologists stand? *Clinical Diabetes and Endocrinology* 5: 69. DOI: 10.1186/s40842-020-00097-1.
10. Ren B, Qin W, Wu F, et al. (2016) Apigenin and naringenin regulate glucose and lipid metabolism, and ameliorate vascular dysfunction in type 2 diabetic rats. *European Journal of Pharmacology* 773: 13–23. DOI: 10.1016/j.ejphar.2016.01.002.
11. Xiao C, Xia ML, Wang J, et al. (2019) Luteolin attenuates cardiac ischemia/reperfusion injury in diabetic rats by modulating Nrf2 antioxidative function. *Oxidative Medicine and Cellular Longevity* 2019. Article ID 2719252.
12. Imran M, Rauf A, Abu-Izneid T, et al. (2019) Luteolin, a flavonoid, as an anticancer agent: a review. *Biomedicine & Pharmacotherapy* 112: 108612. Article 108612.
13. Hayasaka N, Shimizu N, Komoda T, et al. (2018) Absorption and metabolism of luteolin in rats and humans in relation to in vitro anti-inflammatory effects. *Journal of Agricultural and Food Chemistry* 66: 11320–11329.
14. Jegal KH, Kim EO, Kim JK, et al. (2020) Luteolin prevents liver from tunicamycin-induced endoplasmic reticulum stress via nuclear factor erythroid 2-related factor 2-dependent sestrin 2 induction. *Toxicology and Applied Pharmacology* 399: 115036. DOI: 10.1016/j.taap.2020.115036.
15. Özcan FÖ, Aldemir O and Karademir B (2020) Flavones (Apigenin, Luteolin, Crhysin) and their importance for health. *Mellifera* 20(1): 16–27.
16. Kwon EY, Jung UJ, Park T, et al. (2015) Luteolin attenuates hepatic steatosis and insulin resistance through the interplay between the liver and adipose tissue in mice with diet-induced obesity. *Diabetes* 64(5): 1658–1669. DOI: 10.2337/db14-0631.
17. Sangeetha R (2019) Luteolin in the management of type 2 diabetes mellitus. *Current Research in Nutrition and Food Science* 7(2): 393–398. DOI: 10.12944/CRNFSJ.7.2.09.
18. Wang Z, Zeng M, Wang Z, et al. (2021) Dietary luteolin: a narrative review focusing on its pharmacokinetic properties and effects on glycolipid metabolism. *Journal of Agricultural and Food Chemistry* 69(5): 1441–1454. DOI: 10.1021/acs.
19. Xiong C, Wu Q, Fang M, et al. (2020) Protective effects of luteolin on nephrotoxicity induced by long-term hyperglycaemia in rats. *The Journal of International Medical Research* 48(4): 300060520903642. DOI: 10.1177/0300060520903642.
20. Lin Y, Yang N, Bao B, et al. (2020) Luteolin reduces fat storage in caenorhabditis elegans by promoting the central serotonin pathway. *Food and Function* 11: 730–740.
21. Bumke-Vogt C, Osterhoff MA, Borchert A, et al. (2014) The flavones apigenin and luteolin induce FOXO1 translocation but inhibit gluconeogenic and lipogenic gene expression in human cells. *PLoS One* 9(8): e104321. DOI: 10.1371/journal.pone.0104321.
22. Park S, Kim DS, Kang S, et al. (2018) The combination of luteolin and l-theanine improved Alzheimer disease-like symptoms by potentiating hippocampal insulin signaling and decreasing neuroinflammation and norepinephrine degradation in amyloid-β-infused rats. *Nutrition Research Reviews* 60: 116–131. DOI: 10.1016/j.nutres.2018.09.010.
23. Abd-Allah H, Nasr M, Ahmed-Farid OAH, et al. (2020) Nicotinamide and ascorbic acid nanoparticles against the hepatic insult induced in rats by high fat high fructose diet: a comparative study. *Life Sciences* 263: 118540. DOI: 10.1016/j.lfs.2020.118540.
24. Li X, Chen XX, Xu Y, et al. (2022) Construction of glycogen-based nanoparticles loaded with resveratrol for the alleviation of high-fat diet-induced nonalcoholic fatty liver disease. *Biomacromolecules* 23(1): 409–423. DOI: 10.1021/acs.biomac.1c01360.
25. Fan N, Zhao J, Zhao W, et al. (2022) Celastrol-loaded lactosylated albumin nanoparticles attenuate hepatic steatosis in non-alcoholic fatty liver disease. *The Journal of Controlled Release* 347: 44–54. DOI: 10.1016/j.jconrel.2022.04.034.
26. Ganesan P, Ramalingam P, Karthivashan G, et al. (2018) Recent developments in solid lipid nanoparticle and surface-modified solid lipid nanoparticle delivery systems for oral delivery of phyto-bioactive compounds in various chronic diseases. *International Journal of Nanomedicine* 13: 1569–1583. DOI: 10.2147/IJN.S155593.
27. Umrani RD and Paknikar KM (2014) Zinc oxide nanoparticles show antidiabetic activity in streptozotocin-induced Type 1 and 2 diabetic rats. *Nanomedicine (Lond)* 9(1): 89–104. DOI: 10.2217/nnm.12.205.
28. Reed L and Muench H (1938) A simple method of estimating fifty percent end points. *American Journal of Hygiene* 27: 493–497.
29. Bass KF, Gunzel P, Henchler D, et al. (1982) LD50 versus acute toxicity. *Archives of Toxicology* 51: 183–186.
30. Dwivedi DK and Jena GB (2020) NLRP3 inhibitor glibenclamide attenuates high-fat diet and streptozotocin-induced non-alcoholic fatty liver disease in rat: studies on oxidative stress, inflammation, DNA damage and insulin signalling pathway. *Naunyn-Schmiedeberg's Arch Pharmacol* 393(4): 705–716. DOI: 10.1007/s00210-019-01773-5.
31. Matthews DR, Hosker JP, Rudenski AS, et al. (1985) Homeostasis model assessment: IR and beta-cell function from fasting plasma glucose and insulin concentration in man. *Diabetologia* 28: 412–419. DOI: 10.1007/BF00280883.

32. Reitman S and Frankel S (1957) A colorimetric method for the determination of serum glutamic oxalacetic and glutamic pyruvic transaminases. *American Journal of Clinical Pathology* 28(1): 56–63. DOI: 10.1093/ajcp/28.1.56.
33. Allain CC, Poon LS, Chan CSG, et al. (1974) Enzymatic determination of total serum cholesterol. *Clinical Chemistry* 20: 470–475.
34. Fossati P and Prencipe L (1982) Serum triglycerides determined colorimetrically with an enzyme that produces hydrogen peroxide. *Clinical Chemistry* 28: 2077–2080.
35. Lopes-Virella MF, Stone P, Ellis S, et al. (1977) Cholesterol determination in high-density lipoproteins separated by three different methods. *Clinical Chemistry* 23: 882–884.
36. Zhou Y-T, Grayburn P, Karim A, et al. (2000) Lipotoxic heart disease in obese rats: implications for human obesity. *Proceedings of the National Academy of Sciences of the United States of America* 97: 1784–1789.
37. Yoshioka T, Kawada K, Shimada T, et al. (1979) Lipid peroxidation in maternal and cord blood and protective mechanism against activated-oxygen toxicity in the blood. *American Journal of Obstetrics and Gynecology* 135(3): 372–376. DOI: 10.1016/0002-9378(79)90708-7.
38. Beutler E, Duron O and Kelly BM (1963) Improved method for the determination of blood glutathione. *The Journal of Laboratory and Clinical Medicine* 61: 882–888.
39. Srivastava SK and Beutler E (1967) Accurate measurement of oxidized glutathione content of human, rabbit and rat red blood cells and tissues. *Analytical Biochemistry* 25: 70–76.
40. Bełtowski J, Wójcicka G and Jamroz A (2002) Differential effect of 3-hydroxy-3-methylglutaryl coenzyme A reductase inhibitors on plasma paraoxonase 1 activity in the rat. *Polish Journal of Pharmacology* 54(6): 661–671. PMID: 12866722.
41. Livak KJ and Schmittgen TD (2001) Analysis of relative gene expression data using real-time quantitative PCR and the 2(-Delta Delta C(T)) method. *Methods (San Diego, Calif.)* 25(4): 402–408. DOI: 10.1006/meth.2001.1262.
42. Bradford MM (1976) A rapid and sensitive method for the quantitation of microgram quantities of protein utilizing the principle of protein-dye binding. *Analytical Biochemistry* 72: 248–254. DOI: 10.1006/abio.1976.9999.
43. Plaa G, Charbonneau M and Plante I (2014) Detection and evaluation of chemically induced liver injury. In: *Hayes' Principles and Methods of Toxicology*. 6th edition, 1445–1488. DOI: 10.1201/b17359-33.
44. Gastaldelli A and Cusi K (2019) From NASH to diabetes and from diabetes to NASH: mechanisms and treatment options. *JHEP Reports* 1(4): 312–328.
45. Naguib H and Kassab H (2021) Potential relation between non-alcoholic fatty liver disease and glycemic and metabolic parameters in subjects without diabetes. *Egypt Liver Journal* 11: 85. DOI: 10.1186/s43066-021-00154-z.
46. Mahmoud AM, Abdel-Rahman MM, Bastawy NA, et al. (2017) Modulatory effect of berberine on adipose tissue PPARg, adipocytokines and oxidative stress in high-fat diet/streptozotocin-induced diabetic rats. *Journal of Applied Pharmaceutical Science* 7(4): 1–10.
47. Vornoli A, Pozzo L, Della Croce CM, et al. (2014) Drug metabolism enzymes in a steatotic model of rat treated with a high fat diet and a low dose of streptozotocin. *Food and Chemical Toxicology* 70: 54–60. DOI: 10.1016/j.fct.2014.04.042.
48. Oh YS, Baek DJ, Park EY, et al. (2018) Fatty acid-induced lipotoxicity in pancreatic beta-cells during development of type 2 diabetes. *Frontiers in Endocrinology* 9: 384. DOI: 10.3389/fendo.2018.00384.
49. Zhang L, Wang X, He Y, et al. (2022) Regulatory effects of functional soluble dietary fiber from saccharina japonica byproduct on the liver of obese mice with type 2 diabetes mellitus. *Marine Drugs* 20: 91. DOI: 10.3390/md2002009.
50. Bril F, Lomonaco R, Orsak B, et al. (2014) Relationship between disease severity, hyperinsulinemia, and impaired insulin clearance in patients with nonalcoholic steatohepatitis. *Hepatology* 59(6): 2178–2187. Epub 2014 Apr 25. PMID: 24777953. DOI: 10.1002/hep.26988.
51. Lopes R, Santana MS, da Cruz CR, et al. (2020) Central cellular signaling pathways involved with the regulation of lipid metabolism in the liver: a review. *Acta Scientiarum. Biological Sciences* 42: 2020. DOI: 10.4025/actascibiolsci.v42i1.51151
52. Metallo CM, Gameiro PA, Bell EL, et al. (2011) Reductive glutamine metabolism by IDH1 mediates lipogenesis under hypoxia. *Nature* 481: 380–384.
53. Guo S (2014) Insulin signaling, resistance, and the metabolic syndrome: insights from mouse models into disease mechanisms. *The Journal of Endocrinology* 220(2): T1–T23. DOI: 10.1530/joe-13-0327.
54. Gu L, Ding X, Wang Y, et al. (2019) Spexin alleviates insulin resistance and inhibits hepatic gluconeogenesis via the FoxO1/PGC-1α pathway in high-fat-diet-induced rats and insulin resistant cells. *International Journal of Biological Sciences* 15(13): 2815–2829. DOI: 10.7150/ijbs.3178.
55. Xu N, Zhang L, Dong J, et al. (2014) Low-dose diet supplement of a natural flavonoid, luteolin, ameliorates diet-induced obesity and insulin resistance in mice. *Molecular Nutrition & Food Research* 58: 1258–1268.
56. Abdulmalek S, Eldala A, Awad D, et al. (2021) Ameliorative effect of curcumin and zinc oxide nanoparticles on multiple mechanisms in obese rats with induced type 2 diabetes. *Scientific Reports* 11: 20677.
57. Hardy T, Oakley F, Anstee QM, et al. (2016) Nonalcoholic fatty liver disease: pathogenesis and disease spectrum. *Annual Review of Pathology: Mechanisms of Disease* 11: 451–496.
58. Dal S, Van der Werf R, Walter C, et al. (2018) Treatment of NASH with antioxidant therapy: beneficial effect of red cabbage on type 2 diabetic rats *Oxidative Medicine and Cellular Longevity*, 2018: 15. Article ID 7019573. DOI: 10.1155/2018/7019573.
59. Sanders FW and Griffin JL (2016) De novo lipogenesis in the liver in health and disease: more than just a shunting yard for

glucose. *Biological Reviews of the Cambridge Philosophical Society* 91(2): 452–468. DOI: 10.1111/brv.12178.
60. Li D, Guo L, Deng B, et al. (2018b) Long non-coding RNA HR1 participates in the expression of SREBP-1c through phosphorylation of the PDK1/AKT/FoxO1 pathway. *Molecular Medicine Reports* 18: 2850–2856. DOI: 10.3892/mmr.2018.9278.
61. Poulsen MK, Nellemann B, Stødkilde-Jørgensen H, et al. (2016) Impaired insulin suppression of VLDL-triglyceride kinetics in nonalcoholic fatty liver disease. *The Journal of Clinical Endocrinology & Metabolism* 101: 1637–1646.
62. Sun YE, Wang W and Qin J (2018) Anti-hyperlipidemia of garlic by reducing the level of total cholesterol and low-density lipoprotein: a meta-analysis. *Medicine (Baltimore)* 97(18): e0255. DOI: 10.1097/MD.0000000000010255.
63. Berlanga A, Guiu-Jurado E, Porras JA, et al. (2014) Molecular pathways in non-alcoholic fatty liver disease. *Clinical and Experimental Gastroenterology* 7: 221–239. DOI: 10.2147/CEG.S62831.
64. Donnelly KL, Smith CI, Schwarzenberg SJ, et al. (2005) Sources of fatty acids stored in liver and secreted via lipoproteins in patients with nonalcoholic fatty liver disease. *The Journal of Clinical Investigation* 115: 1343–1351.
65. Bechmann LP, Hannivoort RA, Gerken G, et al. (2012) The interaction of hepatic lipid and glucose metabolism in liver diseases. *Journal of Hepatology* 56(4): 952–964. DOI: 10.1016/j.jhep.2011.08.025.
66. Liu G, Zhang Y, Liu C, et al. (2014) Luteolin alleviates alcoholic liver disease induced by chronic and binge ethanol feeding in mice. *The Journal of Nutrition* 144(7): 1009–1015. DOI: 10.3945/jn.114.193128.
67. Zang Y, Igarashi K and Li Y (2016) Anti-diabetic effects of luteolin and luteolin-7-O-glucoside on KK-A(y) mice. *Bioscience, Biotechnology and Biochemistry* 80(8): 1580–1586. DOI: 10.1080/09168451.2015.1116928.
68. Yang X, Wang H, Huang C, et al. (2017) Zinc enhances the cellular energy supply to improve cell motility and restore impaired energetic metabolism in a toxic environment induced by OTA. *Scientific Reports* 7(1): 1–11.
69. Wei CC, Luo Z, Hogstrand C, et al. (2018) Zinc reduces hepatic lipid deposition and activates lipophagy via Zn2+/MTF-1/PPARα and Ca2+/CaMKKβ/AMPK pathways. *Federation of American Societies for Experimental Biology* 18: 6680. DOI: 10.1096/fj.201800463.
70. El-Ashmony SMA, Morsi HK and Abdelhafez AM (2012) Effect of zinc supplementation on glycemic control, lipid profile, and renal functions in patients with type II diabetes: a single blinded, randomized, placebocontrolled, trial. *Journal of Biology, Agriculture and Healthcare* 2(6): 33–41.
71. El-Seidy A, Bashandy S, Ibrahim F, et al. (2022) Zinc oxide nanoparticles characterization and therapeutic evaluation on high fat/sucrose diet induced-obesity. *Egyptian Journal of Chemistry* 65(9): 497–511. DOI: 10.21608/ejchem.2022.112166.5113.
72. John AD, Ragavee A and Selvaraj AD (2020) Protective role of biosynthesised zinc oxide nanoparticles on pancreatic beta cells: an in vitro and in vivo approach. *IET Nanobiotechnology* 14(9): 756–760. DOI: 10.1049/iet-nbt.2020.0084.
73. El-Bahr SM, Shousha S, Albokhadaim I, et al. (2020) Impact of dietary zinc oxide nanoparticles on selected serum biomarkers, lipid peroxidation and tissue gene expression of antioxidant enzymes and cytokines in Japanese quail. *BMC Veterinary Research* 16: 349. DOI: 10.1186/s12917-020-02482-5.
74. Dogra S, Kar AK, Girdhar K, et al. (2019) Zinc oxide nanoparticles attenuate hepatic steatosis development in high-fat-diet fed mice through activated AMPK signaling axis. *Nanomedicine* 17: 210–222. DOI: 10.1016/j.nano.2019.01.013.
75. Cheraghpour M, Imani H, Ommi S, et al. (2019) Hesperidin improves hepatic steatosis, hepatic enzymes, and metabolic and inflammatory parameters in patients with nonalcoholic fatty liver disease: a randomized, placebo-controlled, double-blind clinical trial. *Phytotherapy Research* 33(8): 2118–2125. DOI: 10.1002/ptr.6406.
76. Raza S, Rajak S, Anjum B, et al. (2019) Molecular links between non-alcoholic fatty liver disease and hepatocellular carcinoma. *Hepatoma Research* 5: 42. DOI: 10.20517/2394-5079.2019.014.
77. ALTamimi JZ, Alshammari GM, AlFaris NA, et al. (2022) Ellagic acid protects against non-alcoholic fatty liver disease in streptozotocin-diabetic rats by activating AMPK. *Pharmaceutical Biology* 60(1): 25–37. DOI: 10.1080/13880209.2021.1990969.
78. Ağgül AG, Gür F and Gülaboğlu M (2021) Streptozotocin-induced oxidative stress in rats: the protective role of olive leaf extract. *Bulletin of the Korean Chemical Society* 42: 180–187. DOI: 10.1002/bkcs.12157.
79. Dornas WC, de Lima WG, dos Santos RC, et al. (2012) Salt overload in fructose-fed insulin-resistant rats decreases paraoxonase-1 activity. *Nutrition & Metabolism* 9: 63. DOI: 10.1186/1743-7075-9-63.
80. Adiga U, Banawalikar N and Menambath DT (2022) Association of paraoxonase 1 activity and insulin resistance models in type 2 diabetes mellitus: Cross-sectional study. *Journal of the Chinese Medical Association* 85(1): 77–80. PMID: 35006126. DOI: 10.1097/JCMA.0000000000000665.
81. Papiya B and Singh C (2013) Hepatoprotective activity of luteolin isolated from A. millefolium on CCl4 intoxicated rat. *International Journal of Indigenous Medicinal Plants* 46(4): 1477–1486.
82. Tettey CO and Shin HM (2019) Evaluation of the antioxidant and cytotoxic activities of zinc oxide nanoparticles synthesized using Scutellariabaicalensis root. *Scientific African* 6(e00157): 1–7.
83. Hussein J, El-Naggar ME, Latif YA, et al. (2018) Solvent-free and one-pot synthesis of silver and zinc oxide nanoparticles: activity toward cell membrane component and insulin signaling pathway in experimental diabetes. *Colloids and Surfaces B: Biointerfaces* 170: 76–84.